AIRCRAFT ANGLE-OF-ATTACK VIRTUAL SENSOR DESIGN VIA A FUNCTIONAL POOLING NARX METHODOLOGY*

P.A. Samara, **G.N. Fouskitakis**, **J.S. Sakellariou** *and* **S.D. Fassois**†

Stochastic Mechanical Systems (SMS) Group
Department of Mechanical & Aeronautical Engineering
University of Patras, GR 265 00 Patras, Greece
e-mail: {e_samara,fouskit,sakj,fassois}@mech.upatras.gr
http://www.mech.upatras.gr/∼sms

Keywords: Virtual sensors, identification, aircraft systems.

Abstract

The design of an Angle-of-Attack aircraft Virtual Sensor is pursued via a novel Functional Pooling Nonlinear AutoRegressive with eXogenous excitation (FP-NARX) methodology. This methodology essentially is an identification approach capable of establishing a nonlinear dynamical system model from data obtained from many different flights, each one corresponding to different aircraft and environmental conditions. The FP-NARX model structure is shown to be suitable for Angle-of-Attack Virtual Sensor development within the landing, take-off, and clean flight regimes of the aircraft. Its performance is examined via validation flights, which include substantial aircraft maneuvering, and is shown to be very good, with peak errors not exceeding 1.1 degrees.

1 Introduction

Virtual Sensors (VSs), also referred to as *soft sensors*, are software based devices which utilize measurable signals (Virtual Sensor inputs) in order to reconstruct a signal of interest (Virtual Sensor output). Virtual Sensors are useful in replacing physical sensors, thus reducing hardware redundancy and acquisition cost, or as part of fault detection methodologies by having their output "compared" to that of a corresponding actual sensor.

Although Virtual Sensors may be, in principle, developed based upon mathematical models obtained directly from the physics of the system and first principles, more often than not, such mathematical models are either unavailable, or their exact parameter values are unknown, or they are just too complicated to be used. For this reason the development of Virtual Sensors often has to be based upon identification techniques.

Despite their obvious importance in aerospace applications, where a high level of sensor redundancy is for reliability and safety reasons required, the development of Virtual Sensors has been thus far quite limited. A potential obstacle may have been the highly nonlinear nature of the aircraft dynamics. Virtual Sensors based upon Neural Network (NN) identification has been postulated in a number of recent studies [6, 8, 9, 10, 4]. These Virtual Sensors provide estimates of the signal of interest which is, in many cases, subsequently compared to its counterpart(s) provided by physical sensor(s) in establishing fault diagnosis schemes. Neural Network technology offers the possibility of capturing the nonlinear dynamics of the aircraft, but, on the other hand, it introduces a potentially high level of complexity and time consuming training. Oosterom and Babuska [11] have developed a Virtual Sensor based upon a fuzzy logic model of the Takagi-Sugeno type, which has been successfully applied to the detection of failed physical sensors.

The *goal* of the present study is the design and assessment of an Angle-of-Attack (AoA) Virtual Sensor for a small commercial aircraft through the use of a novel Functional Pooling Nonlinear AutoRegressive with eXogenous excitation (FP-NARX) methodology. This methodology essentially is an identification approach that is capable of overcoming two main difficulties associated with aircraft Virtual Sensor development:

- Capturing the non-linear aircraft dynamics "acting" in a "representative" flight, and,
- Capturing the aircraft behavior under different flights, each one corresponding to different aircraft and environmental conditions.

The FP-NARX methodology consists of two stages: (a) Basic NARX structure determination via a single "representative" flight, and, (b) Functionally Pooled NARX model determination via data obtained from a multitude of flights corresponding to various aircraft and environmental conditions. Although the FP-NARX model follows the generic NARX form (when a single flight is isolated), it does allow for the "expansion' of the basic NARX structure in a physically motivated way.

The Virtual Sensor obtained via a FP-NARX model should be thus capable of reconstructing the Angle-of-Attack (AoA) sig-

*Research supported by the European Commission (Growth Project GRD1-2000-25261, ADFCSII).

†Corresponding author.

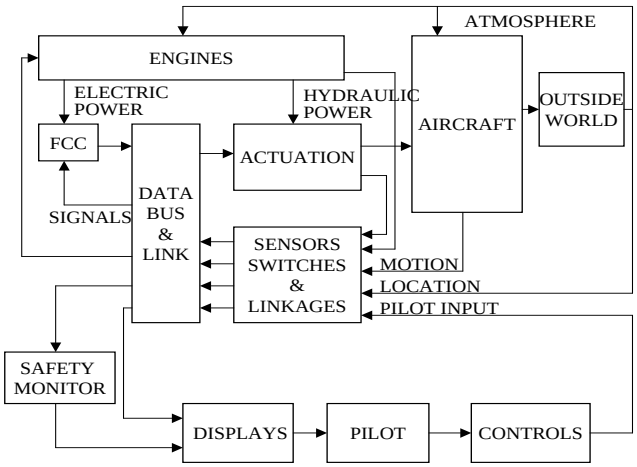

Figure 1: Functional diagram of the aircraft model [3].

nal for any flight and under any environmental conditions. The assessment of the designed AoA Virtual Sensor performance is based upon its ability to reconstruct the signal of interest in a variety of cases and with validation flights (flights not used in estimation).

The rest of this paper is organized as follows: A brief description of the synthetic (simulation) environment of the small commercial aircraft used in the study is presented in Section 2. The Functional Pooling NARX design methodology is presented in Section 3, and its application to AoA Virtual Sensor design in Section 4. The designed Virtual Sensor is assessed in Section 5, and the conclusions drawn from this study are summarized in Section 6.

2 Overview of the aircraft model

The study is based upon a detailed aircraft model implemented within the $\mathrm{MATLAB/Simulink^{TM}}$ environment (synthetic environment). The functional diagram of the model is presented in Figure 1 [2, 3].

The Aircraft block represents the aircraft's nonlinear dynamics using a six degree-of-freedom model. It calculates the total (aerodynamic, engine, gravitational) forces and moments, and computes the resulting accelerations along the body axes, as well as the corresponding angular rates. The inputs to this block are: The wind and/or turbulence, engine thrust, aerodynamic forces and moments obtained from primary (elevators, ailerons, rudder) and secondary (flaps, slats, stabilizers, airbrakes) surfaces, the land gear mechanism, and the aircraft configuration (weight, geometry). The Flight Control Laws block implements the control laws in a parametrized way, allowing for the selection of various gain scheduling strategies.

The Actuation System block describes the nonlinear behavior of the aircraft's primary and secondary actuators. The Pilot block generates the desired pilot actions and transforms the pilot commands into surface commands (deflections). Engine dynamics is modelled by a first-order system in order to produce the corresponding thrust (forces and/or moments). The Outside World block includes the wind and turbulence effects. Turbulence is generated on-line via Dryden type second-order filters (Dryden spectra) [3], and its intensity may be selected as light, moderate, or severe.

The Sensors Block includes three Sensor Modules providing digitized sensor signals. Each module is equipped with appropriate sensor transducers and transducer failure modes. Two of the Sensor Modules include an Air Data Computer (ADC), an Attitude Heading System (AHS), and pilot command sensors, while the third one is equipped with a Global Positioning System (GPS) and an Air Data Computer (ADC). Two Airflow Direction Indicators (ADI) are located directly opposite and aligned, one on each side of the fuselage. This allows for the computation of an estimate of the Angle-of-Attack (AoA). Each ADI measures the local airflow direction at the vane location, and each ADI vane has two position transducers in order to provide independent information to each one of the two ADCs. Each Sensor Module is equipped with a standard Voter/Monitor (V/M) fault detection and isolation block. The basic sampling frequency of the overall system is $50\ Hz$, although certain subsystems run at different frequencies.

3 The Functional Pooling NARX (FP-NARX) Design Methodology

The Functional Pooling NARX (Nonlinear AutoRegressive with eXogenous excitation) methodology postulated for Virtual Sensor design is an identification procedure aiming at establishing a dynamical system model from data obtained from many different flights, each one corresponding to potentially different aircraft and environmental conditions. The methodology consists of two *phases*:

(a) Basic NARX structure determination,

(b) Functionally Pooled NARX model determination.

3.1 Basic NARX structure determination

In order to account for the highly nonlinear dynamical relationships between the signal under reconstruction (virtual sensor output) and the measurable signals used for this purpose (virtual sensor inputs), a stochastic Multiple-Input Single-Output (MISO) Nonlinear AutoRegressive with eXogenous excitation (NARX) model structure of polynomial form is adopted.

The MISO NARX polynomial model structure is of the form:

$$\begin{aligned} y[t] = \theta_0 + \sum_{i_1} \theta_{i_1} \varphi_{i_1}[t] + \sum_{i_1,i_2} \theta_{i_1 i_2} \varphi_{i_1}[t] \varphi_{i_2}[t] + \\ \ldots + \sum_{i_1,\ldots,i_l} \theta_{i_1 \ldots i_\ell} \varphi_{i_1}[t] \ldots \varphi_{i_\ell}[t] + e[t] \Longrightarrow \\ \Longrightarrow \quad y[t] = \sum_{i=0}^{L} \vartheta_i \cdot p_i[t] + e[t] \end{aligned} \tag{1}$$

where t designates normalized discrete time ($t = 1, 2, \ldots, N$), N the data length, $y[t]$ the Virtual Sensor output, and $e[t]$ the

model error assumed to be a zero mean uncorrelated sequence. The terms $\varphi_i[t]$ generally are delayed versions of either the output $y[t]$ (autoregressive, AR, terms) or one of the inputs $u_i[t]$ for $i = 1, 2, \ldots$ (exogenous, X, terms). The θ's designate the corresponding model parameters, with the number of indices indicating the number of $\varphi_i[t]$ terms being multiplied together. The AR order, n_y, designates the maximum delay appearing in the model with regard to $y[t]$, while the X order for the i-th input, n_{u_i}, designates the maximum delay appearing in the model with regard to $u_i[t]$.

In the last form of the model, $p_i[t]$ designates the i-th regressor, generally being a monomial consisting of products of various $\varphi_i[t]$'s. Let the maximum degree of nonlinearity of $p_i[t]$ $(i = 1, 2, \ldots, L)$ be l, and note that $p_0[t] \triangleq 1$ (constant term). In this representation the model parameter corresponding to the i-th regressor is designated as ϑ_i.

In the present (first) phase of the methodology, the basic NARX model structure is determined via a single ("representative") flight. Since the NARX model of equation (1) is linear in the parameters, estimation, based upon minimization of a quadratic function of the error, may be achieved via linear regression. The forward orthogonal least squares estimator [5, 1] is a computationally efficient procedure for determining the terms to be included in the model (model structure). Indeed, the orthogonality property of this estimator results in a particular simple structure determination procedure, which is based upon an auxiliary model defined such that the terms in it are orthogonal to each other over the data set. According to this procedure the determination of the model structure is accomplished via the Error Reduction Ratio (ERR) criterion:

$$\text{ERR}_i = \frac{\sum_{t=1}^{N} g_i^2 \, w_i^2[t]}{\sum_{t=1}^{N} y^2[t]} \times 100\% \tag{2}$$

with $w_i[t]$ and g_i designating the i-th regressor and the corresponding parameter of the auxiliary model, respectively. The quantity ERR provides an indication of which term should be included in the model by assessing the percentage contribution of the $w_i[t]$ regressor to the reduction of the total mean-squared prediction error [5]. Each auxiliary coefficient g_i can be estimated sequentially and independently, which is advantageous when estimating nonlinear models with large numbers of candidate terms.

Since the objective of the present study is the design of a Virtual Sensor, the simulation capability is also important, and for this reason the following Structure Determination Criterion (SDC) is used:

$$\text{SDC}_i = \alpha \cdot \text{ERR}_i + \beta \cdot \delta(\text{NMSE})_i \tag{3}$$

where α and β are selected constants and $\delta(\text{NMSE})_i$ designates the reduction in the Normalized Mean Square Simulation Error when the i-th term is added to the model. The NMSE is defined as follows:

$$\tilde{e}[t] \triangleq y[t] - y_{sim}[t] \tag{4}$$

$$\text{NMSE} = \frac{\| \tilde{e}[t] \|^2}{\| y[t] \|^2} \times 100\% \tag{5}$$

with $y_{sim}[t]$ designating the model-based simulated signal, $y[t]$ the actual signal, and $\|\cdot\|$ Euclidean norm. The selection procedure incorporates those terms which provide a significant SDC. Finally note that the ERR_i and $\delta(\text{NMSE})_i$ terms in SDC_i may be also computed as averages over a number of flights.

3.2 Functionally Pooled NARX model determination.

The basic NARX model structure developed through data obtained from a single "representative" flight and the procedure of the previous subsection may be confirmed as *inadequate* for representing the aircraft dynamics under various flights.

The Functionally Pooled NARX (FP-NARX) model structure aims at overcoming this difficulty by postulating a model suitable for all flight conditions and estimated from data obtained from multiple flights (under different aircraft and environmental conditions).

The first step in developing the FP-NARX model structure is based upon the observation that the basic NARX model parameters are flight dependent. This implicitly indicates the inadequacy of the basic NARX structure under multiple flight scenarios, and is, of course, unacceptable within the present context. The approach postulated for overcoming this difficulty is based upon modification of the basic NARX structure by allowing the model parameters to be functions of measurable flight quantities, say $\ell_1[t], \ell_2[t], \ldots, \ell_q[t]$. Based on this, the model of equation (1) may be expressed as:

$$y[t] = \sum_{i=0}^{L} \vartheta_i(\ell_1[t], \ell_2[t], \ldots, \ell_q[t]) \cdot p_i[t] + e[t] \tag{6}$$

with the ϑ_i's presently being of the form:

$$\vartheta_i(\ell_1[t], \ell_2[t], \ldots, \ell_q[t]) = a_{i_0} + \sum_{j=1}^{r_1} a_{i_{1,j}} \cdot \ell_1^j[t] + \\ + \sum_{j=1}^{r_2} a_{i_{2,j}} \cdot \ell_2^j[t] + \ldots + \sum_{j=1}^{r_q} a_{i_{q,j}} \cdot \ell_q^j[t] \tag{7}$$

with $a_{i_{s,j}}$ designating the coefficient of projection of the i-th model parameter on the $\ell_s^j[t]$ functions. Albeit this model structure follows the generic NARX form when a single flight is isolated, it does allow for the "expansion" of the basic form in a physically motivated way as it permits the use of physical insight in the selection of the measurable quantities affecting the original model parameters.

The model of equation (6) may be re-written as [1]:

$$y[t] = \underbrace{\left[\boldsymbol{p}^T[t] \otimes \boldsymbol{\ell}^T[t]\right]}_{\boldsymbol{\omega}^T[t]} \cdot \boldsymbol{a} + e[t] \tag{8}$$

with:

$$\boldsymbol{p}[t] \triangleq [p_0[t] \ \ldots \ p_L[t]]^T \tag{9}$$

[1] Bold face lower/upper characters designate vector/matrix quantities, respectively.

$$\boldsymbol{\ell}[t] \triangleq \left[1 \vdots \ell_1[t], \ldots, \ell_1^{r_1}[t] \vdots \ldots \vdots \ell_q[t], \ldots, \ell_q^{r_q}[t]\right]^T \quad (10)$$

$$\boldsymbol{a} \triangleq [\boldsymbol{a}_0^T \vdots \boldsymbol{a}_1^T \vdots \ldots \vdots \boldsymbol{a}_L^T]^T \quad (11)$$

$$\boldsymbol{a}_i \triangleq [a_{i_0} \vdots a_{i_{1,1}} \ldots a_{i_{1,r_1}} \vdots \ldots \vdots a_{i_{q,1}} \ldots a_{i_{q,r_q}}]^T \quad (12)$$

with $\otimes$ designating Kronecker product [7, pp. 27–28].

The Functionally Pooled NARX (FP-NARX) model structure, valid for every flight k, may be then specified as follows:

$$y_k[t] = \boldsymbol{\omega}_k^T[t] \cdot \boldsymbol{a} + e_k[t] \qquad (\forall k) \quad (13)$$

$$e_k[t] \sim \text{NID}(0, \sigma_{e_k}^2) \quad (14)$$

$$\text{Cov}[e_k, e_l] = \sigma_{e_k}^2 \cdot \delta_{k,l} \quad (15)$$

$$\boldsymbol{a} : \text{common for all flights (independent of } k) \quad (16)$$

where the subscript k designates the flight, NID$(\cdot,\cdot)$ stands for Normally Independently Distributed with the indicated mean and variance, Cov$[\cdot,\cdot]$ designates covariance of the indicated quantities, and $\delta_{k,l}$ the Kronecker delta ($= 0$ for $i \neq j$, $= 1$ for $i = j$).

Assuming the availability of data of length N ($t = 1, 2, \ldots, N$) from the k-th flight, and employing equation (13), leads to the following matrix equation:

$$\boldsymbol{y}_k = \boldsymbol{\Omega}_k \cdot \boldsymbol{a} + \boldsymbol{e}_k \quad (17)$$

Further assuming the availability of data from a total of M different flights ($k = 1, 2, \ldots, M$) and pooling the equations of the form (17) together (one on top of the other) leads to the expression:

$$\boldsymbol{y} = \boldsymbol{\Omega} \cdot \boldsymbol{a} + \boldsymbol{e} \quad (18)$$

with:

$$\boldsymbol{y} \triangleq \begin{bmatrix} \boldsymbol{y}_1 \\ \boldsymbol{y}_2 \\ \vdots \\ \boldsymbol{y}_M \end{bmatrix} \quad \boldsymbol{\Omega} \triangleq \begin{bmatrix} \boldsymbol{\Omega}_1 \\ \boldsymbol{\Omega}_2 \\ \vdots \\ \boldsymbol{\Omega}_M \end{bmatrix} \quad \boldsymbol{e} \triangleq \begin{bmatrix} \boldsymbol{e}_1 \\ \boldsymbol{e}_2 \\ \vdots \\ \boldsymbol{e}_M \end{bmatrix}$$

A simple estimator for the pooled model parameter vector may be based upon minimization of the trace of the sample error covariance, that is:

$$J \triangleq \text{Trace } \widetilde{\text{Cov}}[\boldsymbol{e}] \quad (19)$$

(the tilde over a quantity indicating sample) which leads to the (suboptimal) Ordinary Least Squares (OLS) estimator for $\boldsymbol{a}$:

$$\hat{\boldsymbol{a}} = \left(\boldsymbol{\Omega}^T \boldsymbol{\Omega}\right)^{-1} \boldsymbol{\Omega}^T \boldsymbol{y} \quad (20)$$

with the hat designating estimator/estimate. Estimates of the various $\sigma_{e_k}^2$'s are subsequently obtained.

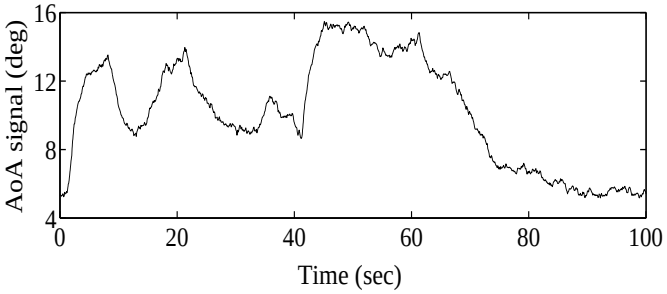

Figure 2: Typical Angle-of-Attack (landing flight regime; light turbulence).

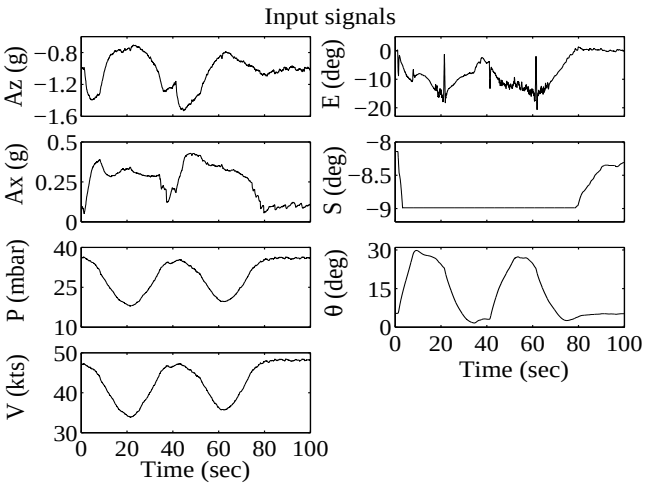

Figure 3: Virtual Sensor input signals for the flight of Figure 2 (landing flight regime; light turbulence).

4 Functional Pooling NARX Design of an AoA Virtual Sensor

The FP-NARX methodology is now used for the design of an Angle-of-Attack (AoA) Virtual Sensor. Preliminary results have indicated that it is beneficial to split the aircraft's flight envelope into three distinct flight regimes, according to Flap/Slat (F/S) configuration (corresponding to landing, $\text{F/S} = 40^o/25^o$, take-off, $\text{F/S} = 20^o/25^o$, and clean flight, $\text{F/S} = 0^o/0^o$), and design a separate Virtual Sensor for each one. The procedure followed for each regime is that of Section 3, with flight data obtained from the simulation model described in Section 2. The flights used are characterized by light turbulence and "sufficient" amounts of aircraft maneuvering through pilot commands on the stick, wheel, and pedal.

4.1 Landing flight regime

Basic NARX structure determination. Within the landing flight regime, basic NARX structure determination is based upon $M = 10$ flights, each one $\Delta t = 90\ sec$ ($N = 4500$ samples) long. The AoA sensor signal for a representative flight is presented in Figure 2.

Various possible Virtual Sensor input signals and NARX structures are considered. Input and model structure selection is

Degree	$\ell = 1$	$\ell = 2$	$\ell = 2$	$\ell = 2$
	Monomial	Monomial	Monomial	Monomial
X term	$p_1[t] = u_1[t-1]$	$p_5[t] = u_2^2[t]$	$p_{11}[t] = u_1[t-1] \cdot u_2[t]$	$p_{17}[t] = u_3[t-1] \cdot u_4[t-1]$
	$p_2[t] = u_3[t-1]$	$p_6[t] = u_5^2[t]$	$p_{12}[t] = u_1[t-1] \cdot u_3[t-1]$	$p_{18}[t] = u_3[t] \cdot u_6[t]$
	$p_3[t] = u_4[t-1]$	$p_7[t] = u_7^2[t]$	$p_{13}[t] = u_1[t-1] \cdot u_4[t-1]$	$p_{19}[t] = u_4[t] \cdot u_6[t-1]$
	$p_4[t] = u_6[t-1]$	$p_8[t] = u_1^2[t-1]$	$p_{14}[t] = u_1[t] \cdot u_7[t]$	$p_{20}[t] = u_5[t-1] \cdot u_6[t-1]$
		$p_9[t] = u_3^2[t-1]$	$p_{15}[t] = u_2[t] \cdot u_4[t]$	$p_{21}[t] = u_6[t-1] \cdot u_7[t]$
		$p_{10}[t] = u_4^2[t-1]$	$p_{16}[t] = u_2[t] \cdot u_6[t]$	
u_1: vertical acceleration (Az), u_2: longitudinal acceleration (Ax), u_3: dynamic pressure (P)				
u_4: true airspeed (V), u_5: elevator (E), u_6: stabilizer (S), u_7: pitch angle (θ)				
AR order: $n_y = 0$ max X order: $n_{u_i} = 1$ delay: $d_i = 0$				
AR terms: 0 X terms: 21 constant term $\neq 0$				
Initial degree of polynomial nonlinearity : $\ell = 2$				
Functional dependencies of the form: $\theta_i\left(u_2[t], u_4[t]\right) = a_{i_0} + a_{i_{1,1}} \cdot u_2[t] + a_{i_{2,1}} \cdot u_4[t] + a_{i_{2,2}} \cdot u_4^2[t]$				
Effective degree of polynomial nonlinearity : $\ell' = 4$				

Table 1: FP-NARX model structure for the landing flight regime.

based upon the methodology described in subsection 3.1 [equation (3); $\alpha = 0.2, \beta = 0.8$] for various flights being included in the model. This procedure leads to the selection of seven Virtual Sensor inputs, as indicated in Table 1. The time histories of these signals, for the flight presented in Figure 2, are presented in Figure 3. The initial NARX degree of polynomial nonlinearity, AR and X orders, as well as input delays, are selected as: $\ell = 2, \quad n_y = n_{u_i} = 1, \quad d_i = 0 \quad (i = 1, \ldots, 7)$, respectively.

The procedure leads to a basic NARX structure characterized by 22 terms, including a constant term (details in Table 1). As $n_y = 0$, the basic NARX model is, in this case, of the Finite Impulse Response type.

Functionally Pooled NARX model determination. The Functional Pooling procedure is based upon $M = 30$ different flights characterized by light turbulence and $\Delta t = 90\ sec$ ($N = 4500$ samples) duration. The procedure leads to a FP-NARX model with parameters being polynomial functions of $u_2[t]$ (longitudinal acceleration) and $u_4[t]$, $u_4^2[t]$ (true airspeed and its square). The final Virtual Sensor model has an effective polynomial degree of $\ell' = 4$ (details in Table 1).

4.2 The take-off and clean flight regimes

Similar FP-NARX model structures are selected for the other two regimes. The Virtual Sensor inputs and basic NARX structure (ℓ, n_y, n_{u_i}, d_i) are the same as in the landing flight regime.

5 AoA Virtual Sensor Assessment

AoA Virtual Sensor assessment is, for the landing flight regime, based upon data obtained during 28 additional flights characterized by light turbulence and $\Delta t = 100\ sec$ ($N = 5000$ samples) duration. The results corresponding to a typical validation flight are presented in Figure 4 which presents the actual AoA, the Virtual Sensor based AoA, and their discrepancy (error) during a large (15.2 degrees) AoA working range.

The performance of the AoA Virtual Sensor with a typical validation flight from within the take-off flight regime is presented in Figure 5, while a summary of the results corresponding to all three flight regimes is presented in Figure 6. This summary indicates the maximum values of the Mean Simulation Error (MSE) and Peak Simulation Error (PSE) for all training (estimation) and all validation flights in each regime. The MSE and PSE quantities are defined as:

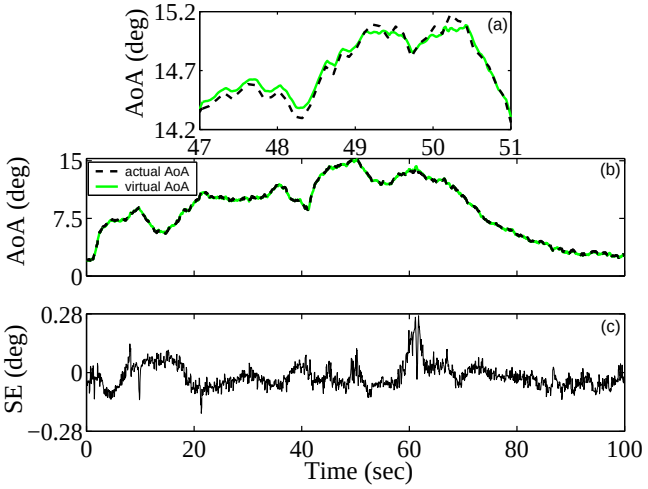

Figure 4: AoA Virtual Sensor performance for a validation flight within the landing flight regime: (a) detail, (b) complete flight, (c) simulation error (−− actual AoA, — Virtual Sensor AoA).

$$\text{MSE} = \max_k \left(\frac{1}{N} \sum_{t=1}^{N} | \ \tilde{e}_k[t] \ | \right) \tag{21}$$

$$\text{PSE} = \max_{k,t} \left(| \ \tilde{e}_k[t] \ | \right) \tag{22}$$

in which k designates the k-th flight within each flight regime and $\tilde{e}[t]$ the simulation error [equation (4)]. It is obvious that the performance of the developed AoA Virtual Sensor is very good in all three flight regimes, with the peak error not exceeding 1.1 degrees.

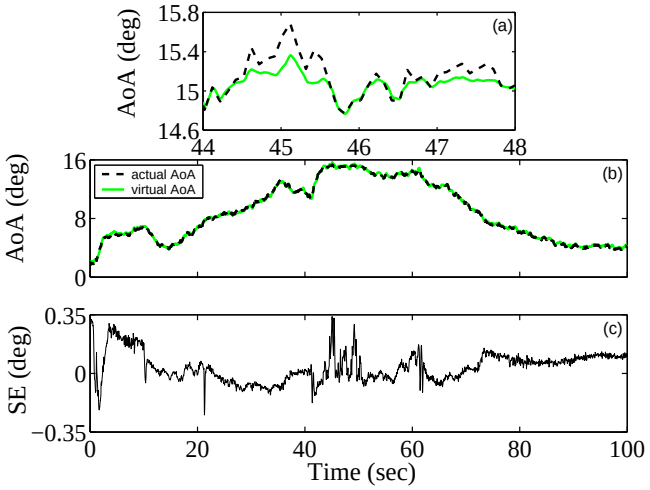

Figure 5: AoA Virtual Sensor performance for a validation flight within the take-off flight regime: (a) detail, (b) complete flight, (c) simulation error (−− actual AoA, — Virtual Sensor AoA).

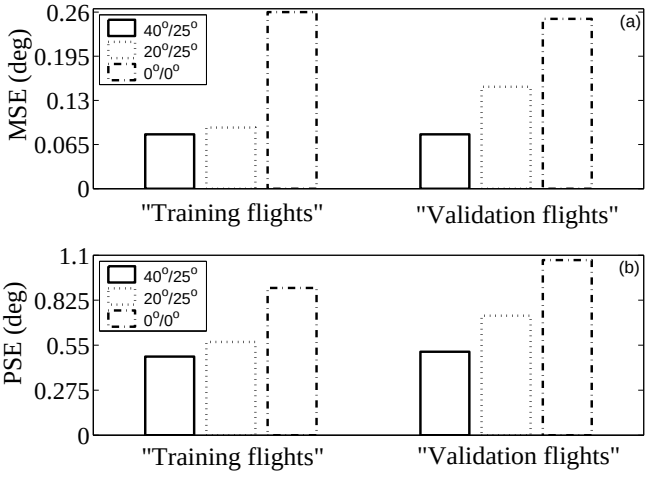

Figure 6: Summary results on AoA Virtual Sensor performance: (a) maximum values of the Mean Simulation Error, (b) maximum values of the Peak Simulation Error (training and validation flights in all flight regimes).

6 Concluding Remarks

The design of an aircraft Angle-of-Attack aircraft Virtual Sensor via a novel Functional Pooling Nonlinear AutoRegressive with eXogenous excitation (FP-NARX) methodology has been presented. This methodology is capable of establishing a nonlinear dynamical system model from data obtained from many different flights, each one corresponding to different aircraft and environmental conditions.

The AoA Virtual Sensor developed for each one of the landing, take-off, and clean flight regimes of the aircraft has been assessed via validation flights, which include substantial aircraft maneuvering, and has been shown to offer very good performance over a wide AoA working range and various flight and environmental conditions. The peak error, in any regime, has not exceeded 1.1 degrees.

Acknowledgements

This research was financially supported by the European Commission (Growth Project GRD1-2000-25261, ADFCSII). The authors are grateful to the partners of the project for providing the aircraft simulation model, as well as for their continual support, comments, and encouragement.

References

[1] S.A. Billings, S. Chen, M.J. Korenberg. “Identification of MIMO non-linear systems using a forward-regression orthogonal estimator”, *Int. J. Control*, **49(6)**, pp. 2157-2189, (1989).

[2] U. Ciniglio, L. Verse. “ADFCS bare aircraft simulation yools: model description and user manual”, *Technical Report*, Centro Italiano Ricerche Aerospaziali (CIRA), Italy, CIRA-TR-98-112, (1999).

[3] U. Ciniglio, L. Verse. “ADFCS fly-by-wire architecture simulation model: user manual”, *Technical Report*, Centro Italiano Ricerche Aerospaziali (CIRA), Italy, CIRA-TR-SIV-99-099, (1999).

[4] D. Goff, R.P. Jones, C. Massey. “Implementation of a neural network based airspeed estimator applicable to an EH101 helicopter”, *Proceedings of the European Control Conference*, pp. 757-761, (2001).

[5] M.J. Korenberg, S.A. Billings, Y.P. Liu, P.J. McIlroy. “Orthogonal parameters estimation algorithm for non-linear stochastic systems”, *Int. J. Control*, **48(1)**, pp. 193-210, (1988).

[6] C. Latorre, B. Tranchero. “Neural net-based virtual sensors in flight control systems”, 15^{th} *IFAC Symposium on Automatic Control in Aerospace*, Bologna, Italy, pp. 416-421, (2001).

[7] J.R. Magnus, H. Neudecker. *Matrix Differential Calculus*, John Wiley and Sons (1988).

[8] D.L. Mattern, L.C. Jaw, T.-H. Guo, R. Graham, W. McCoy. “Using neural networks for sensor validation”, *34th AIAA/ASME/SAE/ASEE Joint Propulsion Conference and Exhibition*, 98-3547, (1998).

[9] M.R. Napolitano, Y. An, B.A. Seanor. “A fault tolerant flight control system for sensor and actuator failures using neural networks”, *Aircraft Design*, **3**, pp. 103-128, (2000).

[10] M.R. Napolitano, C. Neppach, V. Casdorph, S. Naylor, M. Innocenti, G. Silvestri. “Neural network based scheme for sensor failure detection, identification and accommodation”, *J. of Guidance, Control and Dunamics*, **18(6)**, pp. 1280-1286, (1995).

[11] M. Oosterom, R. Babuska. “Virtual sensor for fault detection and isolation in flight control systems - fuzzy modeling approach”, *Proceedings of the* 39^{th} *IEEE Conference on Decision and Control*, **3**, pp. 2645-2650, (2000).